Journal of Physics: Conference Series **521** (2014) 012003 doi:10.1088/1742-6596/521/1/012003

Investigating individual $Fe_{50}Co_{50}$ alloy nanoparticles using X-ray photo-emission electron microscopy

A. Kleibert[1], **A. Balan**[1], **A. Fraile Rodríguez**[2], **and F. Nolting**[1]

[1]Swiss Light Source, Paul Scherrer Institut, Villigen PSI, CH-5232 Switzerland
[2]Departament de Física Fonamental and Institut de Nanociència i Nanotecnologia (IN2UB), Universitat de Barcelona, E-08028 Barcelona, Spain.

Email: armin.kleibert@psi.ch

Abstract. *In situ* X-ray photo-emission electron microscopy (PEEM) together with X-ray circular magnetic dichroism (XMCD) and complementary *ex situ* scanning electron microscopy (SEM) is used to investigate the properties of individual $Fe_{50}Co_{50}$ alloy nanoparticles in a mass-filtered particle ensemble with a mean size of 12 nm. The data reveal a uniform chemical composition of the particles, but a wide distribution of magnetic properties resulting in a co-existence of superparamagnetic (SPM) and ferromagnetically blocked particles. The ferromagnetic (FM) particles suggest enhanced magnetic energy barriers when compared to the magneto-crystalline anisotropy energy (MCA) of bulk $Fe_{50}Co_{50}$.

I. Introduction

Magnetic nanoparticles have attracted recently considerable research interest due to their current and prospective applications in spintronics, drug delivery, cancer therapy, multifunctional materials, and ultrahigh density data storage [1,2,3]. The latter require nanomagnets with magnetic energy barriers E_m which prevent thermally driven switching of the magnetization at room temperature together with a large saturation magnetization to promote reading and writing information at smaller bit sizes [4]. CoPt or FePt alloys in their chemically ordered $L1_0$ phase provide the required properties. In particular, they possess a high MCA providing a respectively high E_m, but they are difficult to prepare at the nanoscale [5]. More recently, the use of FeCo alloys was proposed, which have only small MCA in the bcc bulk phase, but can develop an MCA similar to that of FePt when the lattice is tetragonally distorted [4]. Such distortions and an increased MCA have indeed been found in FeCo thin films [6].

Recent investigations on FeCo nanoparticles revealed a high saturation magnetization and indication for enhanced E_m when compared to the bulk MCA of bcc FeCo [7,8]. However, the data were obtained from ensemble measurements and thus, gave no direct insight in the distribution of properties within these ensembles. A significant scattering of properties can for instance arise from size and shape variations, inter-particle interactions, as well as the contact with the surrounding medium and local surface effects of the individual particles [9]. In case of alloys, the situation becomes even more complicated due possible particle-to-particle variations of the composition and chemical order [5]. Recently, it was demonstrated that X-ray PEEM is suitable to probe the chemical composition and magnetic properties of individual nanoparticles [9,10,11]. In this contribution we use

this technique to investigate the distribution of composition and magnetic properties of single FeCo nanoparticles in a mass-filtered particle ensemble.

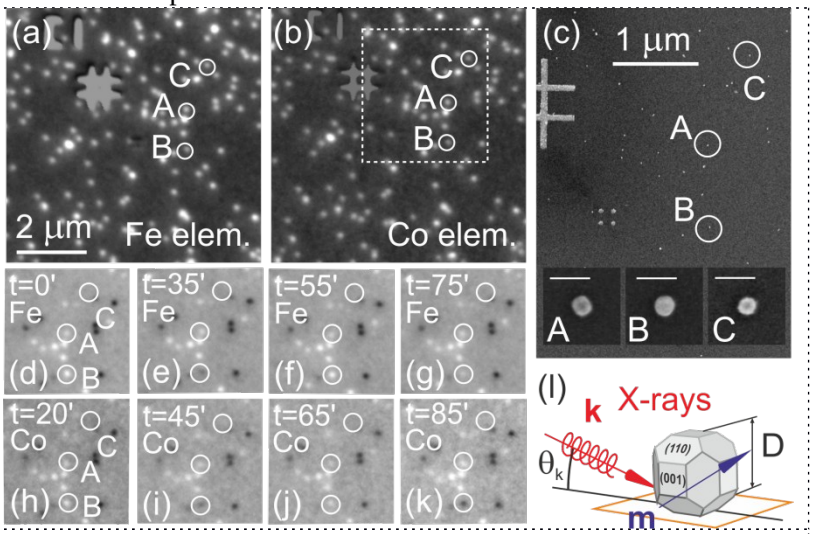

Figure 1. (a),(b) Elemental contrast images recorded at (a) the Fe and (b) the Co L_3 edge. (c) SEM image of the area denoted with the dashed box in (b). The insets show high resolution SEM images of three particles denoted as A, B, and C in (a)-(k). The scale bar in the inset indicates a length of 50 nm. (d)-(g) Magnetic contrast images recorded in the denoted area in (b) as a function of time t (given in minutes) at the Fe L_3 edge. (h)-(k) similar to (d)-(g), but taken at the Co L_3 edge. The particles A, B, C from (b) and (c) are indicated. (l) Sketch of the experimental geometry and the expected equilibrium shape of bcc FeCo nanoparticles.

2. Experimental Details

The nanoparticles are generated in the gas phase by means of an arc cluster ion source using a $Fe_{50}Co_{50}$ alloy target (Vacoflux 50, Vacuumschmelze GmbH) [12]. Mass-filtered particles with a mean size D = 12 nm and size distribution of $\Delta D/D$ = 0.15 [12] are then deposited onto Si wafers with a native oxide layer. A gold mesh is used to measure the particle flux during deposition and to ensure a sufficiently low particle density of a few particles per µm^2 which is required to avoid inter-particle interactions and to enable single particle investigations in our samples. Prior to the particle deposition, the substrates are cleaned by Ar sputtering (20 min, 0.5kV, $5\cdot10^{-5}$ mbar). The elemental composition and the magnetic properties of the particles are studied *in situ* using X-ray PEEM at a base pressure below $5\cdot10^{-10}$ mbar [13]. In the microscope the samples are illuminated at a grazing angle θ_k = 16° with respect to the surface [Fig. 1(f)]. Details on the acquisition of elemental and magnetic contrast maps can be found elsewhere [10,11,14]. All experiments are carried out at room temperature. The particle morphology is studied subsequently to the PEEM experiments by *ex situ* SEM. Lithographic Au/Cr markers on the substrates enable us to identify the same particles in SEM and PEEM.

3. Results and discussion

Elemental contrast maps recorded with X-ray PEEM reveal bright spots at the same sites in images obtained with the photon energy tuned to the Fe and Co L_3 edges, cf. Figs. 1(a) and (b), respectively. Similar to earlier work on size-dependent properties of individual Fe nanoparticles [11,14], most of the bright spots can be assigned to individual nanoparticles with a well-defined, compact shape, as

demonstrated by SEM, cf. Fig. 1(c) and the insets. Clusters of particles and agglomerates are excluded from the analysis. Note that the apparent particles size in SEM is affected (increased) due to the formation of an oxide shell with a thickness of 2-3 nm surrounding the $Fe_{50}Co_{50}$ cores upon sample transfer in ambient air in addition to the limited spatial resolution of the SEM which is about 1 – 2 nm. A detailed correlation of the SEM images with the PEEM elemental contrast maps reveals that every nanoparticle indeed consists of both elements Fe and Co, respectively. Thus, a decomposition of the alloy target material into separate Fe and Co nanoparticles can be excluded.

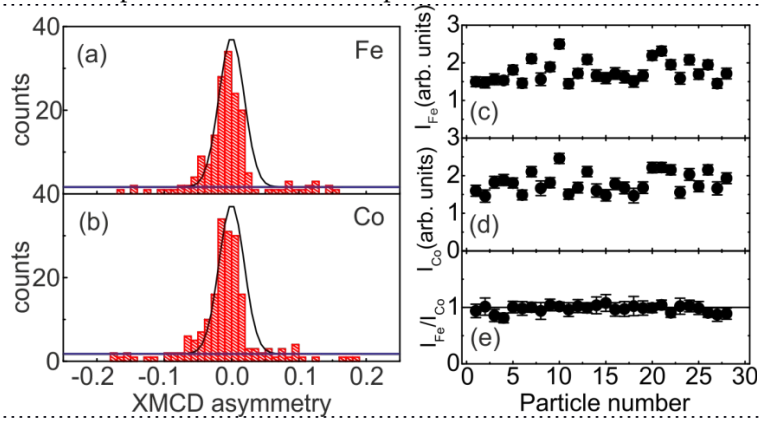

Figure 2. (a),(b) Element-specific histograms of the XMCD asymmetry of individual FeCo nanoparticles. The black and blue lines serve as a guide to the eye. (c),(d) Element-specific intensities I_{Fe} and I_{Co} determined from the elemental contrast maps in Figs. 1(a),(b) for a number of particles.(e) Ratio I_{Fe}/I_{Co} of the same particles.

Examples of element-specific magnetic contrast images, recorded as a function of time in the area denoted in Fig.1(b), are shown in Figs. 1(d)-(k). The magnetic contrast of the particles ranges from black to white through a variety of grey values for both Fe and Co constituents. The magnetic contrast is proportional to the projection of the magnetization m onto the X-ray propagation vector k [11]. Thus, the variety of grey tones reflects a random orientation of the magnetization of the particles due the stochastic deposition process [15]. Some of these particles show stable magnetic contrast over the total observation time which was 9 hours, such as particle ”A” in Fig. 1. The presence of such FM particles is not expected when considering FeCo nanoparticles with bulk-like properties and a highly symmetric equilibrium shape, as schematically shown in Fig.1(l) [12]. Assuming a typical attempt frequency of $1 \cdot 10^{9} s^{-1}$ and using the cubic bulk MCA of FeCo ($K_1 \sim 1 \cdot 10^{4} J/m^3$) in the Arrhenius law for magnetic relaxation, we find that at room temperature only particles with a size larger than about 45 nm should show stable magnetic contrast over the full observation period. This suggests, that the observed FM particles demonstrate significantly modified properties when compared to the above model assumptions.

Closer inspection of the data reveals also the presence of SPM behaviour in a number of particles, which in some cases can be directly observed as changes of sign and magnitude of the magnetic contrast of such particles in time, cf. particle “B” in Figs. 1(d)-(k). The respective fluctuations occur with a rate of a few switching events per hour and thus indicate the onset of SPM behaviour. SPM particles which fluctuate at a much higher rate show no magnetic contrast in all images due to the vanishing average magnetization. Such a case might be presented by particle “C” in Figs. 1(d)-(i). The actual SPM proportion on the sample can be seen, when plotting histograms of the XMCD asymmetry (cf. Ref. [11]) as shown in Figs. 2(a) and (b), where the peak around zero XMCD (indicated by the

black line) reflects the SPM particles (about 60% of the ensemble). The flat part (indicated by the blue line) can be assigned to the FM particles with random orientation of m. Notably the histograms for Fe and Co are similar, as expected from an alloy with well coupled Fe and Co moments.

The distribution of chemical compositions can be studied when analyzing the particle intensities in elemental Fe and Co contrast maps [Figs. 1(a) and (b)]. In Figs. 2(c) and (d) we display the respective intensities I_{Fe} and I_{Co} for a number of particles. The data reveal typical particle-to-particle variations of the intensity as discussed in Ref. [14]. However, the ratio I_{Fe}/I_{Co} is almost constant, which indicates a similar amount of Fe and Co in the probed volume of each particle. Note that the ratio I_{Fe}/I_{Co} does not directly reflect the atomic ratio of Fe and Co, since the absorption cross sections of Fe, Co, and the Si substrate at the Fe and Co L_3 edge energies are different.

4. Conclusion

We have used X-ray PEEM to study the composition and magnetic properties of individual FeCo alloy nanoparticles. The data revealed a wide distribution of magnetic energy barriers which result in a coexistence of superparamagnetic and ferromagnetically blocked nanoparticles in a mass-filtered ensemble of particles with a mean size of 12 nm. In contrast, the atomic ratio of Fe and Co in the probed volume of the particles was found to be uniform in the sample. However, local inhomogeneities in the individual nanoparticles are not excluded and might be responsible for the wide distribution of magnetic properties [16]. The ferromagnetic nanoparticles indicate increased magnetic energy barriers when compared to estimates based on the magneto-crystalline anisotropy of bulk FeCo. Further studies are needed to reveal whether the enhanced magnetic energy barriers are indeed due to the proposed tetragonal lattice distortions or due to other effects.

Acknowledgements

Part of this work was performed at the Surface/Interface:Microscopy (SIM) beam line of the Swiss Light Source, Paul Scherrer Institut, Villigen, Switzerland. This project was funded by the Swiss Nanoscience Institute, University of Basel. AFR acknowledges support from the MICIIN “Ramón y Cajal” Programme.

References

[1] Bansmann J, Baker S H, Binns C, Blackman J A, Bucher J P, Dorantes-Dávila J, Dupuis V, Favre L, Kechrakos D, Kleibert A, Meiwes-Broer K H, Pastor G M, Perez A, Toulemonde O, Trohidou K N, Tuaillon J and Xie Y 2005 *Surf. Sci. Rep.* **56** 189

[2] Rusponi S, Cren T, Weiss N, Epple M, Buluschek P, Claude L and Brune H 2003 *Nat. Mater.* **2** 546

[3] Antoniak C, Gruner M E, Spasova M, Trunova A V, Römer F M, Warland A, Krumme B, Fauth K, Sun S, Entel P, Farle M and Wende H 2011 *Nat. Comm.* **2** 528

[4] Burkert T, Nordström L, Eriksson O and Heinonen O 2004 *Phys. Rev. Lett.* **93** 027203

[5] Tournus F, Sato K, Epicier T, Konno T J and Dupuis V 2013 *Phys. Rev. Lett.* **110** 055501

[6] Andersson G, Burkert T, Warnicke P, Björck M, Sanyal B, Chacon C, Zlotea C, Nordström L, Nordblad P and Eriksson O 2006 *Phys. Rev. Lett.* **96** 037205

[7] Getzlaff M, Bansmann J, Bulut F, Gebhardt R K, Kleibert A and Meiwes-Broer K H 2006 *Appl. Phys. A* **82** 95

[8] Getzlaff M, Kleibert A, Methling R, Bansmann J and Meiwes-Broer K H 2004 *Surf. Sci.* **566-568** 332

[9] Kronast F, Friedenberger N, Ollefs K, Gliga S, Tati-Bismaths L, Thies R, Ney A, Weber R, Hassel C, Römer F M, Trunova A V, Wirtz C, Hertel R, Dürr H A and Farle M 2011 *Nano Lett.* **11** 1710

[10] Fraile Rodríguez A, Nolting F, Bansmann J, Kleibert A and Heyderman L J 2007 *J. Magn. Magn. Mater.* **316** 426
[11] Fraile Rodríguez A, Kleibert A, Bansmann J, Voitkans A, Heyderman L J and Nolting F 2010 *Phys. Rev. Lett.* **104** 127201
[12] Kleibert A, Passig J, Meiwes-Broer K H, Getzlaff M and Bansmann J 2007 *J. Appl. Phys.* **101** 114318
[13] Le Guyader L, Kleibert A, Fraile Rodríguez A, El Moussaoui S, Balan A, Buzzi M, Raabe J and Nolting F 2012 *J. Elec. Spectr. Rel. Phen.* **185** 371
[14] Fraile Rodríguez A, Kleibert A, Bansmann J, and Nolting F 2010 *J. Phys. D: Appl. Phys.* **43** 474006
[15] Kleibert A, Voitkans A and Meiwes-Broer K H 2010 *Phys. Rev. B* **81** 073412
[16] Antoniak C, Lindner J, Spasova M, Sudfeld D, Acet M, Farle M, Fauth K, Wiedwald U, Boyen H G, Ziemann P, Wilhelm F, Rogalev A, and Sun S, 2006 *Phys. Rev. Lett.* **97** 117201